DUCTILE RUPTURE OF ALUMINUM SHEETS

W. Brocks [1], J. Besson [2], O. Chabanet [3], D. Steglich [1]

[1] *Institute of Materials Research, GKSS Research Centre, D-21502 Geesthacht, Germany*
[2] *Centre des Materiaux, Ecole des Mines de Paris, France*
[3] *Pechiney CRV, Parc Economique Centr'Alp, F-38341 Voreppe, France*

ABSTRACT

Crack growth resistance of thin aluminium sheets under monotonic loading is studied and numerically simulated. A phenomenological cohesive zone model and the micromechanically based damage model of Gurson are applied. The yield curve is determined from tensile tests on smooth flat specimens, the model parameters describing separation and damage, respectively, are fitted for a Kahn specimen. Both models guarantee transferability of the respective parameters from the small Kahn specimen to a large M(T) specimen. The respective contributions of elastic, plastic and separation energy to the total external work differ significantly for the two specimens. Crack growth is predicted as normal fracture if the common assumptions of symmetry are applied to the FE mesh, whereas the tests show a transition from normal to slant fracture. The general ability of damage models to simulate slant fracture is demonstrated on a Hill specimen.

KEYWORDS

aluminium sheets, fracture resistance, damage models, cohesive zone model, parameter identification, numerical simulation, slant fracture

INTRODUCTION

A realistic assessment of the residual strength of sheet materials, e.g. aluminum panels and shells in aircraft structures, with defects requires methods to experimentally characterize crack growth resistance as well as numerical simulation tools capable of predicting crack initiation and propagation. The global approach to failure uses macroscopic parameters like *J*-integral, CTOD, CTOA, energy disspation etc. [1]. These quantities suffer from a general lack of transferability of fracture resistance data obtained from specimens to large scale structures. The damage mechanics approach, on the other hand, provides a solution for the transferability problem by describing the degradation of the material by additional internal state variables, such as void volume fraction, porosity, micro-crack density, etc. [2]. These models have been applied successfully to predict crack growth in thick-walled structures [3] where a high stress triaxiality triggers the growth of voids. Their application to thin-walled high strength aluminum alloys, however, faces some specific problems:

- the stress triaxiality is much lower than required for the applicability of the respective models,
- the fracture plane often shifts from a normal to a 45° inclined orientation to the applied load,

- rolled sheets generally show an anisotropic behavior with respect to both plastic hardening and void nucleating particles.

In the present contribution, the plasticity and rupture behavior of thin aluminum sheets is characterized by using smooth tensile specimens and Kahn specimens. Three-dimensional finite element simulations of ductile rupture of small specimens are performed using the Gurson-Tvergaard-Needleman model. As this approach does not appear suitable for modeling crack extension in large structures, a two-dimensional simulation using a cohesive zone model is adopted. Finally, the conditions for simulating slant fracture are addressed. Model modifications accounting for anisotropic behavior are applied in [4] but will not be considered here.

MATERIAL AND SPECIMENS

The investigations were performed on rolled 1.73 mm thick sheets of an aluminum alloy of the 2000 series, which is mainly used in aircraft and space industry. The base material is coated by a 50 ÷ 80 μm thick layer of pure aluminum as a protection against corrosion. Second phase particles have been identified by a chemical analysis as iron and copper together with $Al_{12}Mn_2Cu$ segregations, with a total volume fraction of 0.12 %.

Various specimens have been tested to characterize the deformation and fracture behavior of the material, namely smooth, U- and V-notched flat tensile specimens, Kahn-specimens, see Figure 1, and large M(T) specimens. Kahn-specimens have originally been proposed for the investigation of fracture behavior in ship steel plates [5] and were applied for the determination of fracture properties of aluminum sheets, later [6]. They are C(T) like specimens without fatigue crack, $a/W = 0$, of dimensions 35×60 mm^2. Their advantage is their small size which reduces test and material costs in relation to the M(T) specimens of dimensions 760×1350 mm^2. All specimens were loaded in longitudinal orientation. Whereas smooth and notched tensile specimens failed macroscopically unstable, Kahn- and M(T) showed stable crack growth. The crack initiated normal to the loading direction but changed to slant fracture incliced by 45°, see right hand side of Figure 1. The same mechanism was observed on the M(T) specimens.

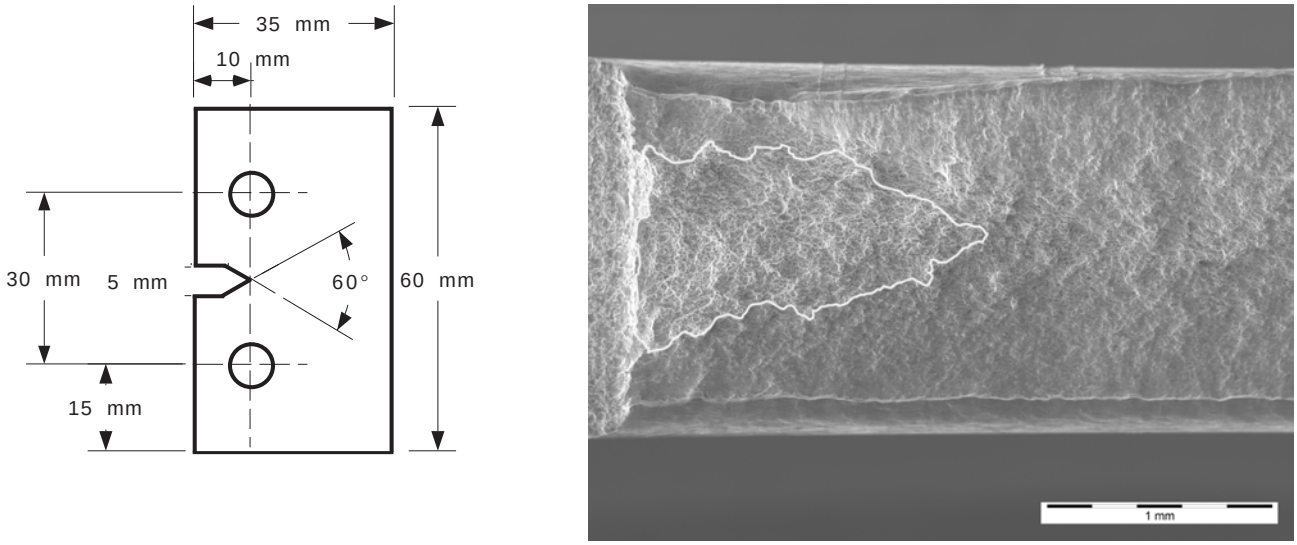

Figure 1: Kahn specimen: size and geometry (left),
fracture surface with normal and slant fracture (right)

MODELS FOR DESCRIBING DUCTILE DAMAGE

The Gurson-Tvergaard-Needleman-Model (GTN)

The model of Gurson [7] for porous metal plasticity with extensions by Tvergaard und Needleman [8] modifies the von Mises yield potential by introducing a damage parameter, f^*, which is a function of the void volume fraction, f,

$$\Phi(\sigma_e,\sigma_h,f,\sigma_Y)=\frac{\sigma_e^2}{\sigma_Y^2\left(\varepsilon^p\right)}+2\,q_1 f^*\cosh\left[q_2\frac{3\,\sigma_h}{2\,\sigma_Y\left(\varepsilon^p\right)}\right]-1-\left(q_1 f^*\right)^2=0 \quad ,$$
$$f^*=\begin{cases} f & \text{for} \quad f\le f_c \\ f_c+\kappa(f-f_c) & \text{for} \quad f>f_c \end{cases} \quad , \tag{1}$$

where σ_e is the von Mises effective stress, σ_h the hydrostatic stress, and $\sigma_Y(\varepsilon^p)$ the actual yield stress of the matrix material. The model was implemented as a "user supplied material" (UMAT) of the FE program ABAQUS.

In accordance with metallographic observations, it is assumed in the present simulations that voids have nucleated with beginning plastic deformation, $f(t=0) = f_0$, and damage evolution occurs due to the growth of

these voids, only. This reduces the number of parameters to five, namely q_1, q_2, f_0, f_c, κ. The parameters $q_1 = 1.5$ and $\kappa = 4$ have the usual values known from literature, whereas $q_2 = 2$ was assumed here for the thin panels with low triaxiality, which differs from common simulations of thick structures. The initial void volume fraction was taken to equal the volume fraction of inclusions, $f_0 = 0.0012$. Coalescence of voids takes place if a critical void volume fraction, f_c, is exceeded, and macroscopic crack growth results from $f^* = 0.6 \approx 1/q_1$. The only adjustable parameter is the critical void volume fraction, f_c.

The Cohesive Zone Model (CZM)

Whereas the GTN model results in constitutive equations governing inelastic deformation and evolution of damage in the continuum, the cohesive zone model intruduces a traction-separation law, $\Sigma(\delta)$, at the "interface" of continuum elements. Hence, the crack has to follow a presecribed path along the element boundaries where cohesive elements have been placed. A decohesion law based on a potential proposed by Rose [9] and applied by Xu and Needleman [10] has been used in the present simulations:

$$\Sigma_n = \sigma_{max}\, e\, z\, \frac{\delta_n}{\delta_c} \exp\left(-z\frac{\delta_n}{\delta_c}\right), \tag{2}$$

with maximum normal stress, σ_{max} and separation length, δ_c , being model parameters; $e = \exp(1)$ and $z = 16\,e/9$ are just numbers. This decohesion law is for pure "mode I" separation, but shear components can be added easily [10]. As the present FE model is 2D and accounts for crack growth in the ligament, only, which is assumed to be a plane of symmetry, no shear stresses can occur and the simulation is restricted to normal fracture. During the separation process, the mechanical work

$$\Gamma_0 = \int_0^{\delta_c} \Sigma_n \,\mathrm{d}\delta_n = \frac{9}{16}\sigma_{max}\,\delta_c \tag{3}$$

is "released". Hence, a crack has grown by one element length if $\delta_n = \delta_c$ or, equivalently, $\Gamma = \Gamma_0$. The CZM has been implemented as "user supplied element" (UEL).

MODELING OF MATERIAL AND SPECIMEN BEHAVIOR

Yield Curve

The yield curve of the material, $\sigma_Y(\varepsilon^p)$, was determined from tensile tests and fitted by a power law,

$$\sigma_Y = \sigma_0 + C\left(\varepsilon^p\right)^n \tag{4}$$

with $\sigma_0 = 343$ MPa, $C = 670$ MPa and $n = 0.67$. Young's modulus was taken as 65 GPa from literature.

Finite Element Models

The global deformation of thin specimens can be well described by plane stress models. The local triaxiality at a crack tip, however, is much higher than in plane stress, $T = 0.66$, as 3D analyses show. As void growth is significantly influenced by stress triaxiality, no damage evolution occurs under plane stress conditions [11] and the GTN model cannot be applied for plane stress elements. Plane strain conditions will overestimate damage evolution on the other hand. Hence, crack growth simulations using the GTN model require a 3D simulation at least in the vicinity of the crack tip and the ligament. In addition, the parameter q_2, which governs the influence of stress triaxiality, see eq. (1), and is commonly set to 1., has to be increased to a value of 2. in the present situation of thin panels. A fourfold symmetry is introduced to reduce the number of elements and unknowns in the FE simulation. Due to this symmetry, damage evolution and crack growth are restricted to a plane normal to the external load, and no slant fracture can be obtained in the simulations.

A 3D model as required for the GTN model is not very convenient for simulations of large amounts of crack growth. The phenomenological CZM offers the advantage of modeling in 2D, as the separation law is not dependent on the local triaxiality. The FE mesh now consists of three regions:

- a process zone where separation occurs, which is modeled by a layer of cohesive elements in the symmetry line, i.e. the ligament,
- a layer of elastic-plastic plane strain elements which allow for higher triaxiality and thus prevent localization of plastic deformation and necking adjacent to the cohesive elements,
- elastic-plastic plane stress elements all over the rest of the specimens, which guarantee the overall plane stress deformation behavior.

Neither of the two models can account for slant fracture. This is due to the symmetry conditions imposed to the 3D simulation with the GTN model, and the restriction to a 2D mesh in the model applying cohesive elements. The simulations have been run under displacement control.

Calibration of Damage Parameters by Simulation of the Kahn Test

The parameters f_c of the GTN model and σ_{max} und δ_c of the decohesion law, respectively, were adjusted to meet the experimental load vs displacement and load vs crack growth curves of the Kahn specimen, see Figure 2. The latter was measured from three specimens for which tests have been stopped at different amounts of crack growth. Both curves are met with satisfactory accuracy by both models, taking $f_c = 0.018$ and $\sigma_{max} = 580$ MPa, $\delta_c = 0.08$ mm, or $\Gamma_0 = 26.1$ N/mm, respectively.

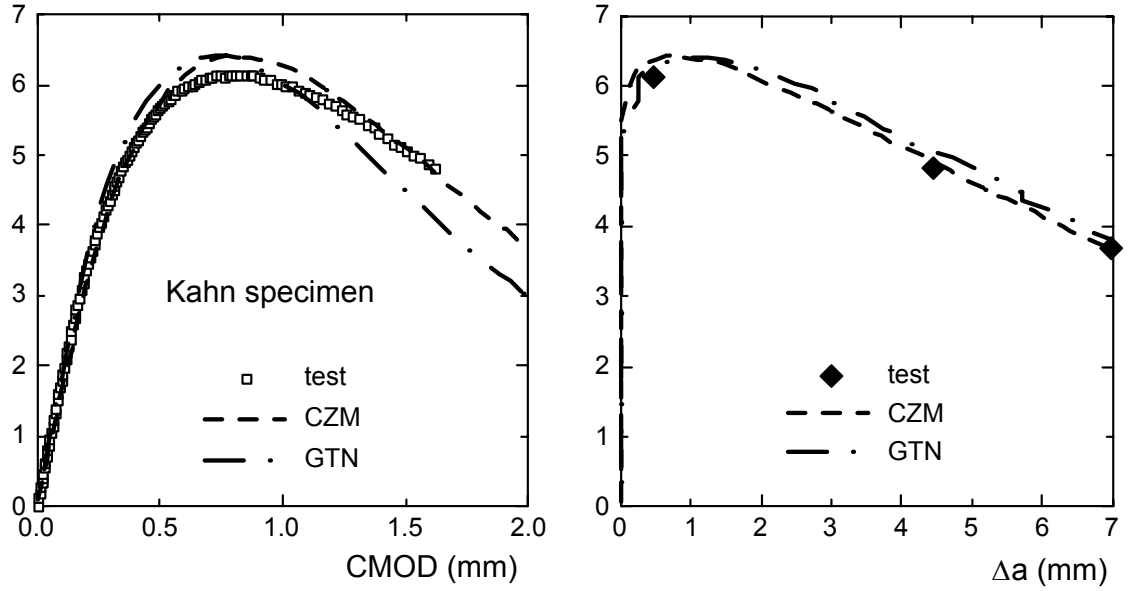

Figure 2: Kahn test and simulation by GTN and CZM

Verification by Simulation of the M(T) Test

The M(T) has now been simulated, taking these parameters, see Figure 3. No perfect agreement between test and simulation results could be obtained. Maximum load is overestimated and reached too early with respect to elongation v_L. On the other hand, crack growth is too fast in the simulation. Keeping in mind that there is a factor of 20 in size between the Kahn and the M(T) specimen, and the former is notched whereas the latter is cracked, the numerical prediction is not too bad. Some additional studies of the involved elastic and dissipated mechanical energies will further elucidate the transfer problems arising between small and large specimens.

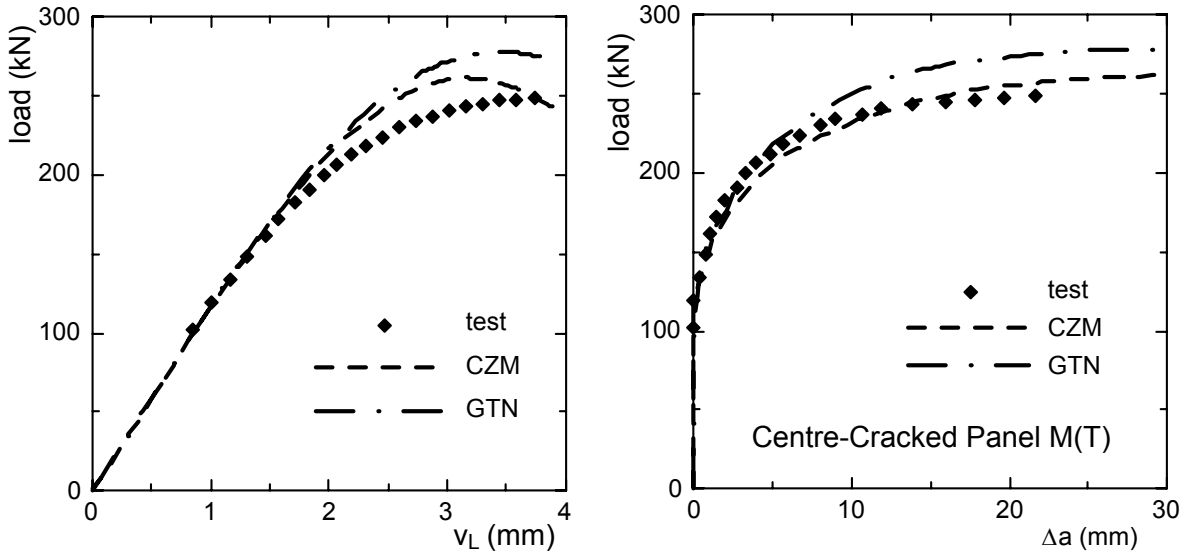

Figure 3: M(T) test and simulation by GTN and CZM

Energy Balances for Kahn and M(T) Specimen

The total external work is either stored as elastic energy or dissipated as work of plastic deformation or work of separation,

$$W = W_{\mathrm{el}} + W_{\mathrm{pl}} + W_{\mathrm{sep}}, \tag{5}$$

with

$$W_{\mathrm{el}} = \int_V \int_0^t \sigma_{ij}\, \dot{\varepsilon}_{ij}^{\mathrm{el}}\, \mathrm{d}t\, \mathrm{d}V, \quad W_{\mathrm{pl}} = \int_V \int_0^t \sigma_{\mathrm{e}}\, \dot{\varepsilon}_{\mathrm{e}}^{\mathrm{pl}}\, \mathrm{d}t\, \mathrm{d}V, \quad W_{\mathrm{sep}} = B\,\Gamma_0\,\Delta a\ . \tag{6}$$

The special advantage of the CZM is that the latter can be separated from the overall work of plastic deformation [12]. An analysis of these contributrions now shows, that plastic work constitutes more than 50 % and up to 70 % of the total mechanical work in the Kahn specimen whereas it is less than 20 % in the M(T) specimen, see Figure 4. Elastic energy amounts to 90 % in the M(T) specimen, but plays a minor role, 20 ÷ 40 %, in the Kahn specimen. Work of separation contributes only 4 % in the Kahn specimen and 0.6 % in the M(T) specimen at maximum crack growth. Thus, what is measured primarily in a J_{R}-curve is plastic work in the Kahn and elastic energy in the M(T) specimen. No wonder that any attempt of transferring these data is senseless. And the really interesting material property of separation energy is not captured at all by the respective tests.

The high amout of elastic energy stored in the M(T) specimen will result in a high influence of Young's modulus on the numerical result. As described above, the panels are not homogeneous but coated with a corrosion protection which comes up to 9 % of the total thickness. A parameter study showed that a reduction of Young's modulus by 9 % reduces maximum load by approximately the same factor. Any influence of the cladding on plastic deformation and dammage has not yet been studied.

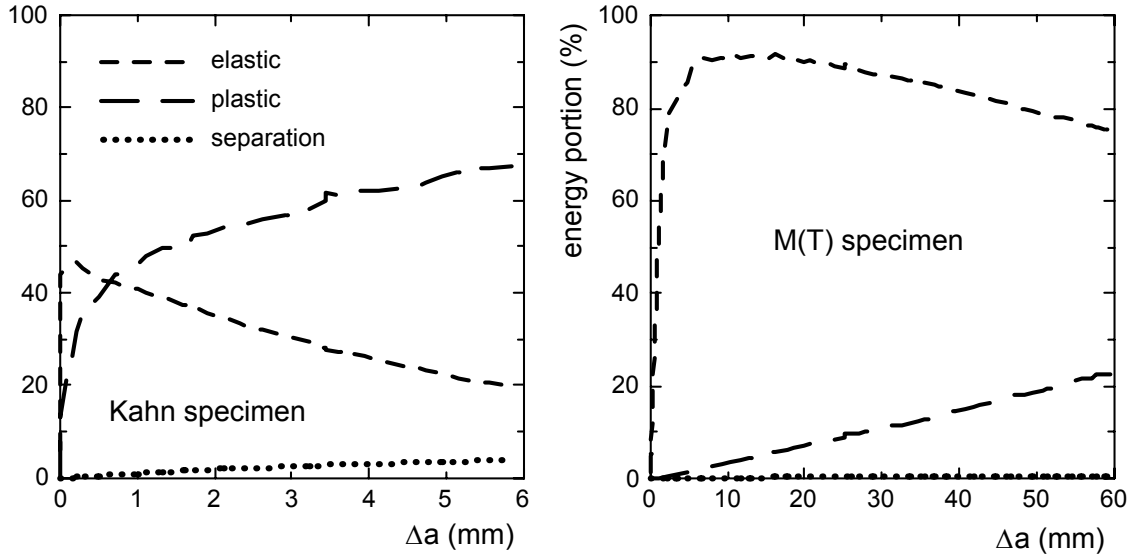

Figure 4: Recoverable and dissipated portions of total external work for Kahn and M(T) specimens

MODELING OF SLANT FRACTURE

As mentioned above and shown in Figure 1, the actual crack plane shifted from a normal to a 45° inclined orientation, which was not accounted for in the two simulations. Damage models as well as cohesive zone models are capable of simulating slant fracture under appropriate modeling conditions, namely

- a full 3D analysis is necessary and no symmetry conditions must be imposed in the ligament,
- the number of elements over the thickness has to be large enough for the models of continuum damage,
- a mode III component has to be added to the separation law and cohesive surface elements have to be placed along the faces of tetrahedral 3D elements to allow for 45° crack paths.

Further details on the influences of meshing and element formulations on the localization behavior of the Gurson [7] and the Rousselier [2] models in the context of modeling slant fracture in flat specimens and cup-cone fracture in round bars are discussed in [4, 13], and an example for modeling slant fracture in a M(T) specimen using cohesive elements is given in [14]. Figure 5 just shows an example of the numerical simulation of slant fracture in a Hill speciman [4] applying the Rousselier model.

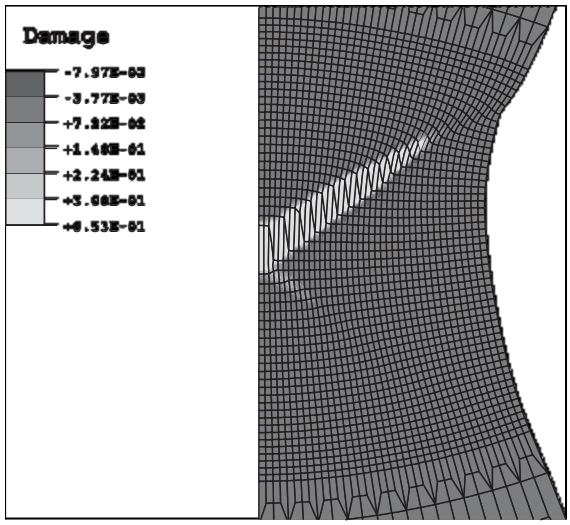

Figure 5: Modeling of slant fracture in the necking section of a Hill specimen by the Rousselier model

CONCLUSIONS

Finite element models with continuum elements incorporating damage evolution as well as cohesive zone elements are capable of simulating ductile rupture of thin aluminum panels. The respective model parameters can be determined from tests on comparably small and simple specimens, namely the Kahn specimen. Both models guarantee transferability over a large range of specimen sizes, though the global balances of mechanical energies differ significantly.

Crack growth is predicted as normal fracture if the common assumptions of symmetry are applied to the FE mesh, whereas tests on thin structures show a transition from normal to slant fracture. In general, damage models as well as cohesive zone models are capable of simulating slant fracture under appropriate modeling conditions. The computational consumption is considerable, however, and inhibits simulation of large amounts of crack growth.

ACKNOWLEDGEMENT

The presented results have been obtained in a cooperation project between PECHINEY CRV and GKSS Research Centre. The authors thank J. Ch. Ehrström, J. Heerens und D. Hellmann for providing the test data.

REFERENCES

1. Harris, C., Newman, J., Piascik, R. and Starnes, J. (1989). J. Aircraft 35, pp. 307-317.
2. Rousselier, G., Devaux, J. C., Mottet, G. and Devesa, G. (1989). Nonlinear Fracture Mechanics: Volume II - Elastic-Plastic Fracture, ASTM STP 995, pp. 332-354.
3. Brocks, W., Klingbeil, D., Künecke, G. and Sun, D.-Z. (1995). in: Second Symp. on Constraint Effects, ASTM STP 1224, pp. 232-252
4. Besson, J., Brocks, W., Chabanet, O. and Steglich, D. (2001). Europ. J. of Finite Elements, to be published.
5. Kahn, N. and Imbembo, E. (1958). The Welding Journal 27, pp. 169-184,.
6. Kaufman, J. and Knoll, A. (1964). Materials Research and Standards 4, pp. 151-155.
7. Gurson, A. L. (1977). J. Engng. Materials and Technology 99, pp 2-15.
8. Needleman, A. and Tvergaard, V.(1984). J. Mech. Phys. Solids 32, pp 461-490.
9. Rose, J., Ferrante, J. and Smith, J. (1981). Phys. Review Letters 47, pp. 675-678.
10. Xu, X. and Needleman, A. (1994). J. Mech. Phys. Solids 42, pp. 1397-1434.

11. Sun, D.-Z., Kienzler, R., Voss, B. and Schmitt, W. (1992). Fracture Mechanics: Twenty-Second Symposium (Volume II), ASTM STP 1131, pp 368-378.
12. Siegmund, Th. and Brocks, W. (2000). Fatigue and Fracture Mechanics: 31st Vol, ASTM STP 1389, pp. 475-485.
13. Besson, J., Steglich, D. and Brocks, W. (2001). Int.. J. of Plasticity, to be published.
14. Brocks,W. (2000). in: Advances in Computational Engineering & Sciences, ICCES 2K, pp.1037-1042.